

**Theoretical study on electron-free-radical scattering: An application to CF**M.-T. Lee,<sup>1</sup> I. Iga,<sup>1</sup> L. M. Brescansin,<sup>2</sup> L. E. Machado,<sup>3</sup> and F. B. C. Machado<sup>4</sup><sup>1</sup>*Departamento de Química, UFSCar, 13565-905 São Carlos, São Paulo, Brazil*<sup>2</sup>*Instituto de Física "Gleb Wataghin," UNICAMP, 13083-970 Campinas, São Paulo, Brazil*<sup>3</sup>*Departamento de Física, UFSCar, 13565-905 São Carlos, São Paulo, Brazil*<sup>4</sup>*ITA, CTA, São José de Campos, São Paulo, Brazil*

(Received 21 December 2001; published 30 July 2002)

In this work, a theoretical study on electron-CF collisions in the low- and intermediate-energy range is reported. More specifically, calculated elastic differential, integral, and momentum-transfer cross sections as well as grand total (elastic and inelastic) and absorption cross sections are presented in the (1–500)-eV energy range. A complex optical potential is used to represent the electron-molecule interaction dynamics, while the Schwinger variational iterative method combined with the distorted-wave approximation is used to solve the scattering equations. Comparison of the present results with existing experimental and theoretical data for electron collisions with NO (an isoelectronic molecule of CF) is made.

DOI: 10.1103/PhysRevA.66.012720

PACS number(s): 34.80.Bm

**I. INTRODUCTION**

Electron-molecule collisions play important role in a number of scientific and technological applications such as lasers, gas discharges, plasmas [1], and magnetohydrodynamics power generation [2]. In particular, the interest on electron interaction with highly reactive radicals such as  $\text{CH}_x$ ,  $\text{CF}_x$  ( $x=1,2,3$ ), etc., has grown recently, in view of their importance in developing plasma devices. It is well known that plasma environment is composed of many species such as electrons, molecules (in their ground and excited states), neutral radicals, ionic fragments, etc. The knowledge of cross sections for electron interaction with these constituents is important in determining the plasma properties and therefore is useful for plasma modelings. In this sense, cross sections for  $e^-$ -CF collisions are particularly relevant, since CF is an important byproduct formed during the process of plasma etching of semiconductors, in which carbon fluoride compounds with general formulas  $\text{C}_n\text{F}_{2n+2}$  are frequently used as reactive gases. Unfortunately, the experimental determination of cross sections for  $e^-$ -CF collisions is difficult. Only recently, electron-impact ionization cross sections of this highly reactive radical were reported in the literature [3]. To our knowledge, there are no other cross-section measurements for electron scattering by this radical. Therefore, a theoretical calculation of such cross sections would contribute to fill this lack of information. Recently,  $e^-$ -radical collisions have been a subject of increasing interest of theoretical investigations. Joshipura and co-workers [4,5] have reported grand total cross sections (TCS's) for electron scattering by several  $\text{CH}_x$ ,  $\text{NH}_x$ , and  $\text{OH}$  radicals in the intermediate- and high-energy range. More recently, Baluja and co-workers reported a  $R$ -matrix calculation of elastic and excitation cross sections for low-energy electron collisions with  $\text{ClO}$  [6] and  $\text{CH}$  [7]. Nevertheless, to date, the only theoretical study for  $e^-$ -CF scattering was performed by Kim and Irikura [8]. In their work, electron-impact total ionization cross sections (TICS's) of CF were calculated using the binary-encounter Bethe (BEB) model for incident energies up to 10 keV. However, their calculated TICS's in the

(15–200)-eV range lie significantly above the experimental results of Deutsch *et al.* [3].

In this work, we present a theoretical study on electron scattering by the CF radical in the low- and intermediate-energy range. Specifically, calculated elastic differential, integral, and momentum-transfer cross sections (DCS's, ICS's, and MTCS's) as well as TCS's and total absorption cross sections (TACS's) are presented for electron-impact energies ranging from 1 to 500 eV. In our study, a complex optical potential was used to describe the dynamics of  $e^-$ -CF interaction, while a combination of the Schwinger variational iterative method (SVIM) [9,10] and the distorted-wave approximation (DWA) [11–13] is used to solve the scattering equations. This procedure has already been successfully applied to treat electron scattering by a number of molecules [14–18] and thus we expect that it can also be useful for  $e^-$ -radical collisions. Although the present study is unable to provide directly TICS's, our calculated TACS's provide an estimate of the contributions of all inelastic collisions including both excitation and ionization processes. Joshipura *et al.* [5] have observed that for a set of molecules the ionization dominates the inelastic processes, the values of the TICS's being about 80% of the TACS's at energies around 100 eV and about 100% for energies above 300 eV. Particularly for the  $e^-$ -CF collision, some light could be shed through the comparison with the corresponding process for  $\text{CF}_4$ . For the latter, Christophorou and Olthoff [19] have observed that the values of the TICS's also correspond to about 80% of the TACS's for incident energies above 50 eV. Therefore, the present calculated TACS's provide an upper limit of the TICS's for this radical and their comparison with experimental and calculated TICS's is expected to be meaningful. On the other hand, due to the lack of experimental results of other types of cross sections for  $e^-$ -CF collisions, we compare our calculated results with the experimental [20,21] and calculated data [22] for electron scattering by NO, which is isoelectronic of CF.

The organization of this paper is as follows: In Sec. II, we describe briefly the theory used and also give some details of the calculation. In Sec. III, we compare our calculated results

with experimental and theoretical data for  $e^-$ -NO scattering available in the literature. A brief conclusion remark is also presented in this section.

## II. THEORY AND CALCULATION

Since the details of the SVIM and the DWA have already been presented in previous works [9–13], only a brief outline of the theory will be given here. The wave functions  $\Psi_k^\pm(\vec{r})$  of the scattering electron are solutions of the well-known Lippmann-Schwinger integral equation,

$$\Psi_k^\pm(\vec{r}) = \Phi_k(\vec{r}) + G_0^\pm U_{int} \Psi_k^\pm(\vec{r}), \quad (1)$$

where  $\vec{k}$  is the linear momentum of the scattering electron,  $\Phi_k(\vec{r})$  is a plane-wave function,  $G_0$  is an unperturbed Green's operator, and  $U_{int} = 2V_{int}$  is the reduced electron-target interaction potential. In Eq. (1), the superscripts (+) and (−) denote the outgoing-wave and incoming-wave boundary conditions, respectively.

In the present study, the electron-molecule scattering dynamics is represented by a complex optical potential, given by

$$V_{int}(\vec{r}) = V^{SEP}(\vec{r}) + iV_{ab}(\vec{r}), \quad (2)$$

where  $V^{SEP}$  is the real part of the interaction potential formed by static ( $V_{st}$ ), exchange ( $V_{ex}$ ), and correlation-polarization ( $V_{cp}$ ) contributions, whereas  $V_{ab}$  is an absorption potential.  $V_{st}$  and  $V_{ex}$  are obtained exactly from a Hartree-Fock self-consistent-field (SCF) target wave function. A parameter-free model potential introduced by Padial and Norcross [23] is used to account for the correlation-polarization contributions. In this model, a short-range correlation potential between the scattering and the target electrons is defined in an inner region and a long-range polarization potential in an outer region. The first crossing of the correlation and polarization potential curves defines the inner and the outer regions. The correlation potential is calculated by a free-electron-gas model, derived from the target electronic density according to Eq. (9) of Padial and Norcross [23]. In addition, the asymptotic form of the polarization potential is used for the long-range electron-target interaction. Calculated dipole polarizabilities using a single and double configuration interaction target wave function,  $\alpha_0 = 10.01$  a.u. and  $\alpha_2 = 2.55$  a.u., were used to generate the asymptotic  $V_{cp}$ . No cutoff or other adjusted parameters are needed for the calculation of  $V_{cp}$ .

The absorption potential  $V_{ab}$  in Eq. (2) is given as

$$V_{ab}(\vec{r}) = -\rho(\vec{r})(T_L/2)^{1/2}(8\pi/5k^2k_F^3) \times H(\alpha + \beta - k_F^2)(A + B + C), \quad (3)$$

where

$$T_L = k^2 - V^{SEP}, \quad (4)$$

$$A = 5k_F^3/(\alpha - k_F^2), \quad (5)$$

$$B = -k_F^3[5(k^2 - \beta) + 2k_F^2]/(k^2 - \beta)^2, \quad (6)$$

and

$$C = 2H(\alpha + \beta - k^2) \frac{(\alpha + \beta - k^2)^{5/2}}{(k^2 - \beta)^2}. \quad (7)$$

In Eqs. (3)–(7),  $k^2$  is the energy (in Rydbergs) of the incident electron,  $k_F$  the Fermi momentum, and  $\rho(\vec{r})$  the local electronic density of the target.  $H(x)$  is a Heaviside function defined by  $H(x) = 1$  for  $x \geq 0$  and  $H(x) = 0$  for  $x < 0$ . According to Staszewska *et al.* [24],

$$\alpha(\vec{r}, E) = k_F^2 + 2(2\Delta - I) - V^{SEP}, \quad (8)$$

and

$$\beta(\vec{r}, E) = k_F^2 + 2(I - \Delta) - V^{SEP}, \quad (9)$$

where  $\Delta$  is the average excitation energy and  $I$  is the ionization potential.

The Lippmann-Schwinger scattering equation for elastic  $e^-$ -CF collisions is solved using the SVIM considering only the real part of the optical potential. In SVIM calculations, the continuum wave functions are single center expanded as

$$\Psi_k^\pm(\vec{r}) = \left[ \frac{2}{\pi} \right]^{1/2} \sum_{lm} \frac{(i)^l}{k} \Psi_{klm}^\pm(\vec{r}) Y_{lm}(\hat{k}). \quad (10)$$

The absorption part of the  $T$  matrix is calculated via the DWA as

$$T_{abs} = i \langle \Psi_f^- | V_{ab} | \Psi_i^+ \rangle. \quad (11)$$

Once both the real and the imaginary parts of the  $T$  matrix are known, the cross sections for  $e^-$ -CF collisions can be promptly calculated. Since CF is a polar molecular radical, a fixed-nuclei treatment for this problem is known [25] to lead to divergent DCS's in the forward direction, due to the slow falloff of the partial-wave  $T$ -matrix elements for large  $l$ . Consequently, the calculated ICS's and TCS's would also diverge for all incident energies. This divergence can be removed only with the introduction of the nuclear motion in the Hamiltonian. In order to overcome these difficulties, we made use of the adiabatic-nuclei-rotation (ANR) framework to calculate rotational excitation cross sections. Then, DCS's for rotationally unresolved elastic  $e^-$ -CF collisions are calculated by summing the individual rotational excitation cross sections up to convergence.

Within the ANR, the DCS's for the excitation from an initial rotational level  $j_0$  to a final level  $j$  is given by

$$\frac{d\sigma}{d\Omega}(j \leftarrow j_0) = \frac{k_j}{k_0} \frac{1}{(2j_0 + 1)} \sum_{m_j m_{j_0}} |\langle j m_j | f | j_0 m_{j_0} \rangle|^2, \quad (12)$$

where  $j_0, m_{j_0}$  ( $j, m_j$ ) are the rotational quantum numbers of the initial (final) rotational state,  $f$  is the laboratory-frame (LF) electronic part of the scattering amplitude and  $k_0$  and  $k_j$  are the linear momentum magnitudes of the incident and the

scattered electron, respectively. Using the rigid-rotor approximation, the wave function for a given  $|jm_j\rangle$  is

$$|jm_j\rangle = \left[ \frac{(2j+1)}{8\pi^2} \right]^{1/2} D_{m_j,0}^j(\hat{R}), \quad (13)$$

where  $D_{m_j,0}^j$  are the usual finite rotational matrix elements.

The partial-wave expansion of the rotational excitation scattering amplitude is given by

$$\begin{aligned} \langle jm_j | f | j_0 m_{j_0} \rangle &= 4\pi [(2j+1)(2j_0+1)]^{1/2} \\ &\times \sum_{ll'm} (-1)^{m+m_{j_0}+1} i^{l-l'} T_{ll'm} Y_{l'm_j-m_{j_0}} \\ &\times \sum_L (2L+1)^{-1} (l0l'm_j-m_{j_0} | ll' L m_j \\ &- m_{j_0}) (l-m_l'm | ll' L 0) \\ &\times (j-m_j j_0 m_{j_0} | jj_0 L m_{j_0}-m_j) \\ &\times (j_0 j_0 0 | jj_0 L 0), \end{aligned} \quad (14)$$

where  $T_{ll'm}$  are the scattering  $T$ -matrix elements,  $Y_{lm}$  the usual spherical harmonics, and  $(l_1 m_1 l_2 m_2 | l_1 l_2 l_3 m_3)$  are Clebsch-Gordan coefficients.

The rotationally summed DCS's are then calculated as

$$\frac{d\sigma}{d\Omega} = \sum_{j=0} \frac{d\sigma}{d\Omega} (j \leftarrow j_0). \quad (15)$$

Since CF is an open-shell radical with the ground-state configuration  $X^2\Pi$ , two spin-specific scattering channels, namely, those leading to the singlet and to the triplet couplings between the scattering electron and the isolated  $2\pi$  electron of the target, are considered in the present study. Therefore the statistical average of the elastic-scattering DCS's is written as

$$\frac{d\sigma}{d\Omega} = \frac{1}{4} \left[ 3 \left( \frac{d\sigma}{d\Omega} \right)^1 + \left( \frac{d\sigma}{d\Omega} \right)^0 \right], \quad (16)$$

where  $(d\sigma/d\Omega)^1$  and  $(d\sigma/d\Omega)^0$  are the multiplet-specific DCS's averaged over molecular orientations for the total ( $e^- + \text{CF}$ ) spin  $S=1$  (triplet) and  $S=0$  (singlet) couplings, respectively.

In this study, a standard  $[10s5p/4s3p]$  basis set of Dunning [26] augmented by one  $d$  ( $\alpha=0.8$ ) uncontracted function for the carbon atom and four  $p$  ( $\alpha=0.12, 0.06, 0.03$ , and  $0.015$ ), and one  $d$  ( $\alpha=1.58$ ) uncontracted functions for the fluorine atom is used for the calculation of the SCF target wave function. At the experimental equilibrium geometry of the ground-state CF ( $R=2.400$  a.u.), this basis set yielded the calculated SCF energy of  $-137.206048$  a.u. and the dipole moment of  $0.0473$  a.u. The experimental dipole moment for this radical is  $0.254$  a.u. [27].

In the present study, we have limited the partial-wave expansion of the continuum wave functions as well as of the  $T$ -matrix elements up to  $l_{\max}=30$  and  $m_{\max}=17$ . In view of

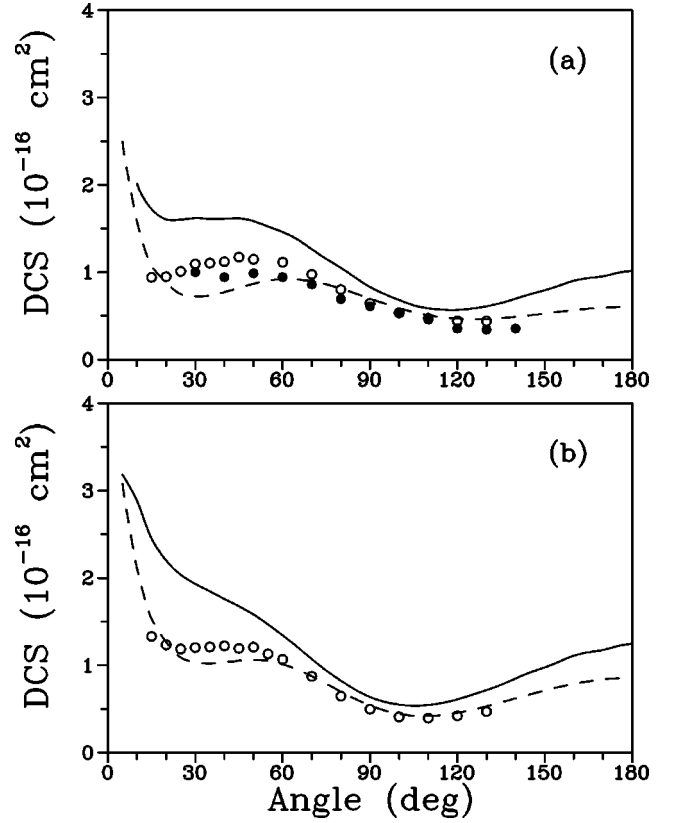


FIG. 1. DCS's for elastic  $e^-$ -CF scattering at (a) 5 eV and (b) 7.5 eV. Full curve, present rotationally summed results; dashed line, calculated DCS's for  $e^-$ -NO scattering of Fujimoto and Lee [22]; open squares, experimental data for elastic  $e^-$ -NO scattering of Mojarrabi *et al.* [21]; full circles, experimental data for elastic  $e^-$ -NO scattering of Kubo *et al.* [20].

the smallness of the CF permanent dipole moment, these partial-wave-expansion parameters already provide quite good convergence. Nevertheless, in order to obtain a better description for DCS's at the forward direction, a Born-closure formula is used to account for the contribution of higher partial-wave components to the scattering amplitudes. Accordingly, Eq. (14) is rewritten as

$$\begin{aligned} \langle jm_j | f | j_0 m_{j_0} \rangle &= 4\pi [(2j+1)(2j_0+1)]^{1/2} \\ &\times \sum_{ll'm} (-1)^{m+m_{j_0}+1} i^{l-l'} (T_{ll'm} - T_{ll'm}^{\text{Born}}) \\ &\times Y_{l'm_j-m_{j_0}} \times \sum_L (2L+1)^{-1} \\ &\times (l0l'm_j-m_{j_0} | ll' L m_j - m_{j_0}) \\ &\times (l-m_l'm | ll' L 0) (j-m_j j_0 m_{j_0} | jj_0 L m_{j_0}-m_j \\ &- m_j) (j_0 j_0 0 | jj_0 L 0) + \langle jm_j | f^{\text{Born}} | j_0 m_{j_0} \rangle, \end{aligned} \quad (17)$$

where  $T_{ll'm}^{\text{Born}}$  are the partial-wave expanded  $T$ -matrix ele-

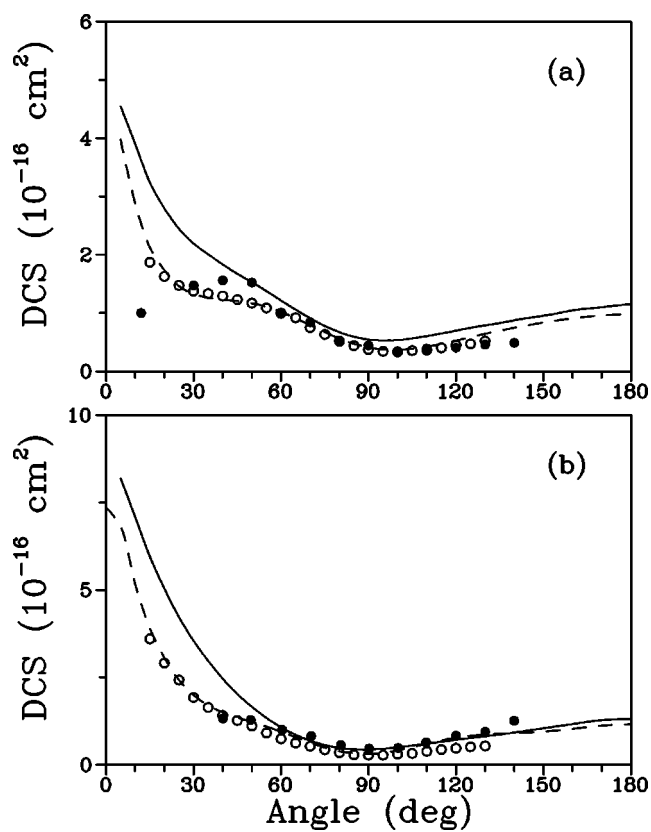


FIG. 2. Same as Fig. 1 but for (a) 10 eV and (b) 15 eV.

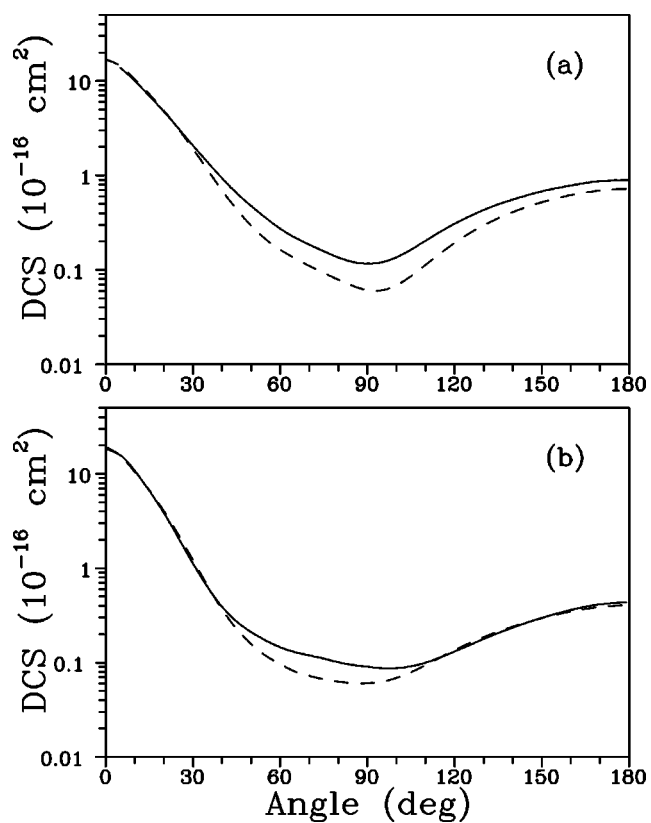


FIG. 4. Same as Fig. 1 but for (a) 50 eV and (b) 80 eV.

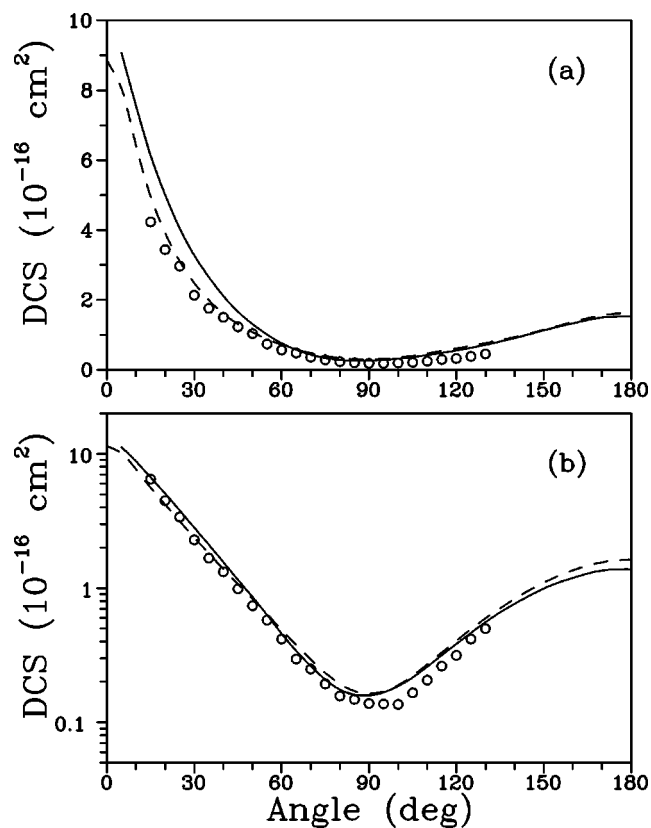


FIG. 3. Same as Fig. 1 but for (a) 20 eV and (b) 30 eV.

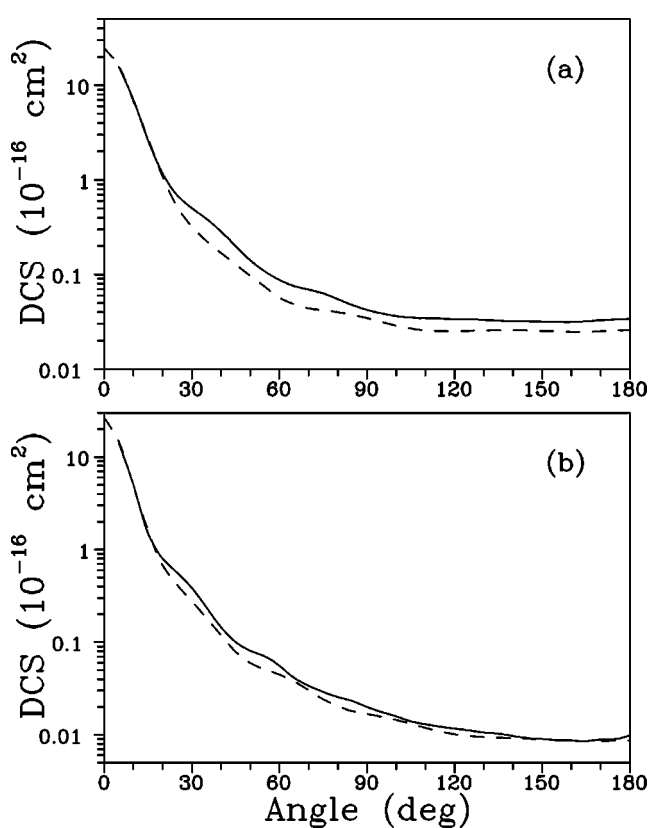


FIG. 5. Same as Fig. 1 but for (a) 300 eV and (b) 500 eV.

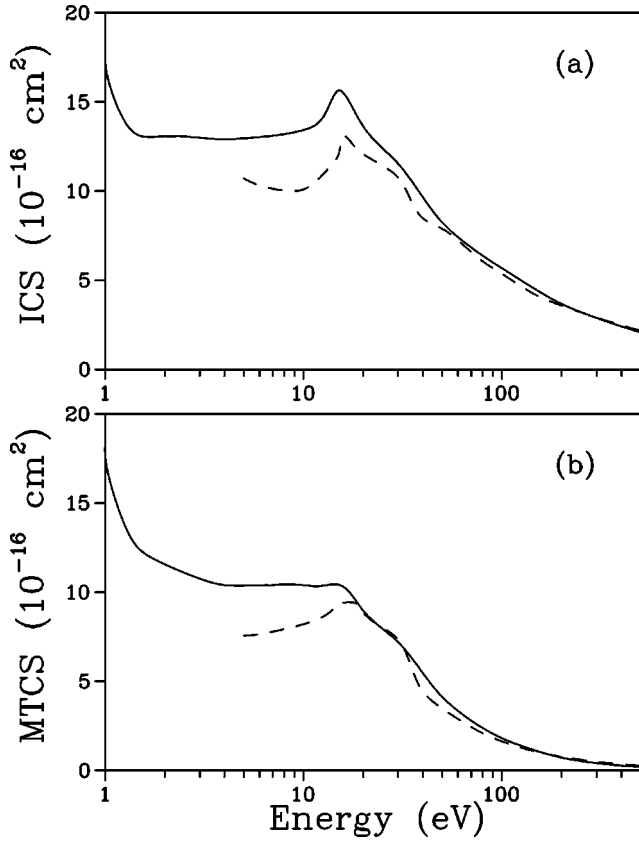


FIG. 6. (a) ICS's and (b) MTCS's for elastic electron scattering by CF in the (1–500)-eV range. The symbols are the same as in Fig. 1.

ments. They are calculated using the first Born approximation. For a rotating dipole, those elements are given by

$$T_{ll'm}^{Born} = -\frac{D}{L} \left[ \frac{(L+m)(L-m)}{(2L+1)(2L-1)} \right]^{1/2}, \quad (18)$$

where  $L=l'$  when  $l'=l+1$  and  $L=l$  when  $l'=l-1$ . In

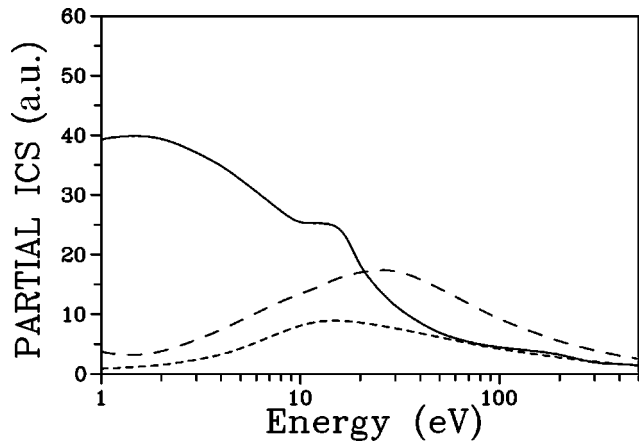


FIG. 7. Partial ICS's, in atomic units ( $a_0$ ), for elastic electron scattering by CF in the (1–500)-eV range. Full curve, results for the  $k\sigma$  scattering channel; dashed curve, for the  $k\pi$  channel; short-dashed curve, for the  $k\delta$  channel.

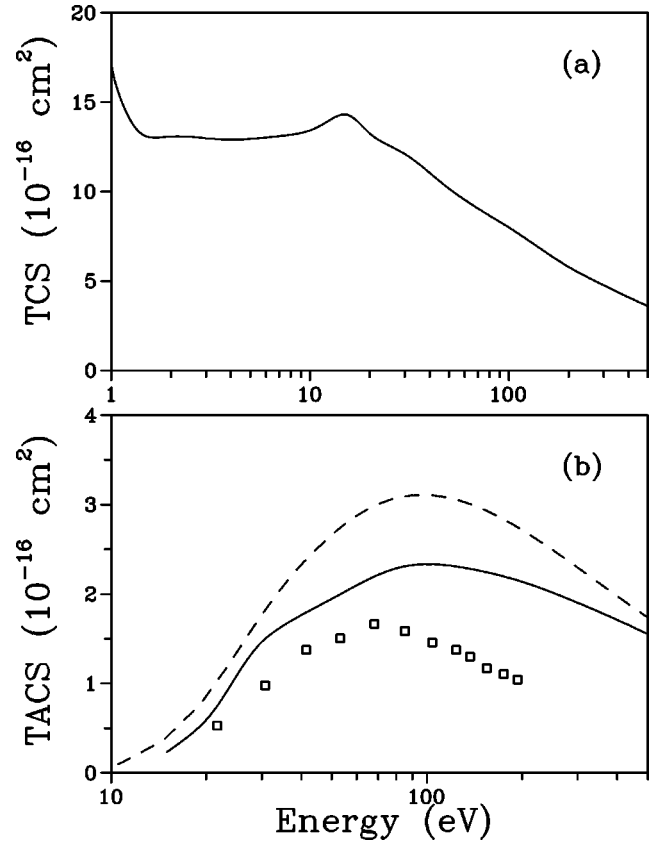


FIG. 8. (a) TCS's and (b) TACS's for electron scattering by CF in the (1–500)-eV range. Full curve, present calculated results, dashed line, the BEB TICS's of Kim and Irikura [8]; open squares, experimental TICS's of Deutsch *et al.* [3].

addition, for  $j_0=0$ , the full LF Born electron-scattering amplitude for a rotating dipole with dipole moment  $D$  is given by

$$f^{Born} = \frac{2D}{q} \left[ \frac{4\pi}{3} \right]^{1/2} i \sum_m D_{m0}^1(\hat{R}) Y_{1m}(\hat{q}'), \quad (19)$$

where  $\vec{q}' = \vec{k}_0' - \vec{k}_f'$  is the LF momentum transferred during the collision. The calculated HF dipole moment of CF is used in Eqs. (18) and (19). In summing up the contributions of individual rotational excitation cross sections, sufficient terms were included to ensure the convergence to be within 0.2%. In addition, the TCS's are calculated by using the optical theorem and the TACS's were taken as the difference between calculated TCS's and ICS's.

### III. RESULTS AND DISCUSSION

In Figs. 1–5 we present our calculated rotationally summed DCS's for elastic  $e^-$ -CF scattering in the (5–500)-eV energy range. Due to the lack of experimental or other calculated DCS's for elastic electron scattering by this radical, we compare our results with some available calculated [22] and experimental [20,21] data for  $e^-$ -NO collisions. Since NO is an isoelectronic molecule of CF, some



similarities on the cross sections of electron scattering by these targets are expected. In fact, a general good agreement between the DCS's for  $e^-$ -CF and  $e^-$ -NO collisions is seen in the (20–500)-eV energy range. This similarity has also been observed for electron scattering by other isoelectronic target pairs such as CO and N<sub>2</sub> [28,29]. Nevertheless, at lower incident energies ( $E_0 \leq 15$  eV), the calculated DCS's for  $e^-$ -CF collisions are larger than those for  $e^-$ -NO collisions, particularly for scattering angles  $\theta \leq 60^\circ$ .

Figures 6(a) and 6(b) show our ICS's and MTCS's, respectively, calculated in the (1–500)-eV range. The comparison is again made with the calculated results for  $e^-$ -NO collisions [22] for the same reason as before. On qualitative aspects, the ICS's and MTCS's for both targets show a resonance feature centered at around 15 eV. This feature is due to the occurrence of a shape resonance in the  $k\sigma$  scattering channel as can be seen in the partial ICS's for  $e^-$ -CF collisions, shown in Fig. 7. The resonance seen in the ICS's of  $e^-$ -NO collisions probably has the same origin. Quantitatively, a very good agreement between the ICS's and the MTCS's for electron scattering by CF and NO is observed for incident energies above 20 eV. Nevertheless, at lower incident energies, again the calculated results for CF lie systematically above than those for NO.

It is known that HF calculations are, in general, unable to reproduce accurate dipole moments for molecules with small and/or moderate permanent dipole moment, such as CO, NO, N<sub>2</sub>O, etc. Despite that, HF molecular wave functions have been widely used in electron-molecule scattering calculations. In view of the substantial discrepancy between the calculated HF and the experimental value of the dipole moment for the CF radical, some test runs were made using the experimental value of  $D$  in Eqs. (18) and (19), in order to verify its influence on the calculated DCS's, mainly near the

forward direction. It was found that the resulting discrepancy in the DCS's is lower than 5% at a scattering angle of  $5^\circ$  and an incident energy of 10 eV. This difference becomes much smaller for both larger scattering angles and higher energies. As a result, the discrepancies in the corresponding ICS's are about 3% at 10 eV and less than 1.0% at 100 eV and above.

Figures 8(a) and 8(b) show our calculated TCS's in the (1–500)-eV energy range and TACS's in the (15–500)-eV energy range, respectively, for the  $e^-$ -CF collisions. Experimental [3] and calculated [8] TICS's are also shown in Fig. 8(b) for comparison. In general, there is a qualitative agreement between the present calculated TACS's and those results available for comparison. Quantitatively, our calculated TACS's lie between the experimental TICS's of Deutsch *et al.* and the calculated TICS's of Kim and Irikura. As stated before, our calculated TACS's are in fact an upper limit of the TICS's. If we assume that the ionization contribution is about 80% in the energy range covered herein, we can conclude that our calculations are capable to provide estimates for TICS's that are in reasonable agreement with the experimental values. In view of the simplicity of the model potential used here, this fact is quite encouraging.

Considering the scarceness of both theoretical and experimental cross sections for electron scattering by this important radical, it is hoped that the results reported in the present study can be useful for scientific and technologic applications, particularly in plasma modelings.

## ACKNOWLEDGMENTS

This work was partially supported by the Brazilian agencies FAPESP, CNPq, and FINEP-PADCT.

- 
- [1] J. Hahn and C. Junge, *Z. Naturforsch. A* **32A**, 190 (1977).
  - [2] W. Wang and N.D. Sze, *Nature (London)* **286**, 589 (1980).
  - [3] H. Deutsch, T.D. Märk, V. Tarnosky, K. Becker, C. Cornelissen, L. Cospiva, and V. Bonacic-Koutescky, *Int. J. Mass Spectrom. Ion Processes* **137**, 77 (1994).
  - [4] K.N. Joshipura and M. Vinodkumar, *Phys. Lett. A* **224**, 361 (1997).
  - [5] K.N. Joshipura, M. Vinodkumar, and P.M. Patel, *J. Phys. B* **34**, 509 (2000).
  - [6] K.L. Baluja, N.J. Mason, L.A. Morgan, and J. Tennyson, *J. Phys. B* **33**, L677 (2000).
  - [7] K.L. Baluja and A.Z. Msezane, *J. Phys. B* **34**, 3157 (2001).
  - [8] Y.-K. Kim and K.K. Irikura, in *Atomic and Molecular Data and Their Applications*, edited by K. Barrington and K.L. Bell, AIP Conf. Proc. No. 543 (AIP, Melville, New York, 2000), p. 220.
  - [9] R.R. Lucchese, G. Raseev, and V. McKoy, *Phys. Rev. A* **25**, 2572 (1982).
  - [10] L. Mu-Tao, L.M. Brescansin, M.A.P. Lima, L.E. Machado, and E.P. Leal, *J. Phys. B* **23**, 4331 (1990).
  - [11] A.W. Fliflet and V. McKoy, *Phys. Rev. A* **21**, 1863 (1980).
  - [12] M.-T. Lee and V. McKoy, *Phys. Rev. A* **28**, 697 (1983).
  - [13] M.-T. Lee, S. Michelin, L.E. Machado, and L.M. Brescansin, *J. Phys. B* **26**, L203 (1993).
  - [14] M.-T. Lee, I. Iga, L.E. Machado, and L.M. Brescansin, *Phys. Rev. A* **62**, 062710 (2000).
  - [15] M.-T. Lee and I. Iga, *J. Phys. B* **32**, 453 (1999).
  - [16] L.E. Machado, E.M.S. Ribeiro, M.-T. Lee, M.M. Fujimoto, and L.M. Brescansin, *Phys. Rev. A* **60**, 1199 (1999).
  - [17] I. Iga, M.G.P. Homem, K.T. Mazon, and M.-T. Lee, *J. Phys. B* **32**, 4373 (1999).
  - [18] S.E. Michelin, T. Kroin, I. Iga, M.G.P. Homem, and M.-T. Lee, *J. Phys. B* **33**, 3293 (2000).
  - [19] L.G. Christophorou and J.K. Olthoff, *J. Phys. Chem. Ref. Data* **28**, 967 (1999).
  - [20] M. Kubo, D. Matsunaga, T. Suzuki, and H. Tanaka, *At. Coll. Res. Jpn.* **7**, 4 (1981).
  - [21] B. Mojarrabi, R.J. Gulley, A.G. Middleton, D.C. Cartwright, P.J.O. Teubner, S.J. Buckman, and M.J. Brunger, *J. Phys. B* **28**, 487 (1995).
  - [22] M.M. Fujimoto and M.-T. Lee, *J. Phys. B* **33**, 4759 (2000).
  - [23] N.T. Padial and D.W. Norcross, *Phys. Rev. A* **29**, 1742 (1984).

- [24] G. Staszewska, D.W. Schwenke, and D.G. Truhlar, Phys. Rev. A **29**, 3078 (1984).
- [25] L.A. Collins and D.W. Norcross, Phys. Rev. A **18**, 467 (1978).
- [26] T.H. Dunning, J. Chem. Phys. **55**, 716 (1971).
- [27] *Handbook of Chemistry and Physics*, edited by D.V. Lide, 73rd ed. (CRC Press, Boca Raton, FL, 1993).
- [28] R.D. Dubois and M.F. Rudd, J. Phys. B **9**, 2657 (1976).
- [29] J.P. Bromberg, J. Chem. Phys. **52**, 1243 (1970).